Food Bioscience 57 (2024) 103539

Contents lists available at ScienceDirect

Food Bioscience

journal homepage: www.elsevier.com/locate/fbio

Assessment of the in-vitro toxicity and in-vivo therapeutic capabilities of *Juglans regia* on human prostate cancer and prostatic hyperplasia in rats

Azzurra Stefanucci [a], Lorenza Marinaccio [a], Eulogio J. Llorent-Martínez [b], Gokhan Zengin [c], Onur Bender [d], Rumeysa Dogan [d], Arzu Atalay [d], Omotayo Adegbite [e], Foluso O. Ojo [f], Adejoke Y. Onaolapo [g], Olakunle J. Onaolapo [h,**], Adriano Mollica [a,*]

[a] *Department of Pharmacy, University "G. d'Annunzio" of Chieti-Pescara, via deiVestini 31, 66100, Chieti, Italy*
[b] *Department of Physical and Analytical Chemistry, University of Jaén, Campus Las Lagunillas S/N, E-23071, Jaén, Spain*
[c] *Department of Biology, Science Faculty, Selcuk University, 42130, Konya, Turkey*
[d] *Biotechnology Institute, Ankara University, 06135, Ankara, Turkey*
[e] *Department of Pharmacology, Ladoke Akintola University of Technology, Ogbomoso, Oyo State, Nigeria*
[f] *Department of Anatomy, Ladoke Akintola University of Technology, Ogbomoso, Oyo State, Nigeria*
[g] *Behavioral Neuroscience Unit, Neurobiology Subdivision, Department of Anatomy, Ladoke Akintola University of Technology, Ogbomoso, 210214, Oyo, Nigeria*
[h] *Behavioral Neuroscience Unit, Neuropharmacology Subdivision, Department of Pharmacology, Ladoke Akintola University of Technology, Ogbomoso, 210214, Oyo, Nigeria*

ARTICLE INFO

Keywords:
Fresh fruits *Juglans regia*
Antioxidants
Cell lines
Prostate
Prostate specific antigen
Phytochemicals

ABSTRACT

Benign prostatic hyperplasia (BPH) and prostatic cancer are aging-associated urological conditions in men. While significant advances have been made in relation to treatment, poor response, treatment resistance and adverse side-effects limit currently available therapies. The possible antiproliferative and/or ameliorative potentials of *Juglans regia* have been reported, however, there is a dearth of scientific information on its effect on BPH or prostatic cancer. In this study, *in-vivo* and *in-vitro* studies were used to assess the possible benefits of fresh walnut fruits extract in BPH or prostate cancer. High-performance liquid chromatography coupled with electro spray ionization and quadrupole-time-of-flight mass spectrometry (HPLC-ESI-Q-TOF) was used to assess the chemical profile of the plant extract. The anti-proliferative activity of *Juglans regia* extract was tested against normal and cancerous human prostate cell lines by using the iCELLigence real-time and label-free cell analysis system. The ameliorative potential of fresh fruits *Juglans regia* extract was assessed by administering the extract at 50 and 100 mg/kg body weight to rats with testosterone induced BPH. Analysis of phytochemicals in *Juglans regia* revealed a high concentration of phenolic acids and flavonoids, *Juglans regia* also showing time- and dose-dependent anti-proliferative activity against prostate cancer cells, and reversed biochemical and histomorphological changes induced by testosterone-induced BPH.

1. Introduction

Nowadays the search for natural sources of bioactive compounds acting against human diseases is at the forefront of modern medicine (Ak et al., 2021; Pieretti et al., 2022). Benign prostatic hyperplasia (BPH) and prostate cancer are two important aging-related diseases of the prostate gland in the modern society, thus the limitations of currently-available therapies necessitate research into novel, cheaper, and possibly less-toxic ones. Although BPH is a multifocal, non-malignant, enlargement of the prostate gland associated with inflammation, fibrosis, alterations in smooth muscle activity causes lower urinary tract symptoms and increases the risk of prostate cancer among other cancers. While significant advances have been made in relation to diagnosis and treatment of BPH, the consistent use of current therapies is limited by poor response, treatment resistance and the development of adverse side effects. Herbs and medicinal plants including willow herb, pumpkin seed, maritime pine bark, rye pollen, tomato, *Pygeum africanum* bark and saw palmetto fruit are particularly useful in the management of BPH largely due to their reduced side effects and high phytochemical content. A number of these beneficial

* Corresponding author.
** Corresponding author.
E-mail addresses: olakunleonaolapo@yahoo.co.uk (O.J. Onaolapo), a.mollica@unich.it (A. Mollica).

https://doi.org/10.1016/j.fbio.2023.103539
Received 10 October 2023; Received in revised form 24 December 2023; Accepted 25 December 2023
Available online 26 December 2023

plants contain active ingredients including phytosterols, β-sitosterol and lectins (Choi et al., 2016; Csikós et al., 2021; Fagelman & Lowe, 2002), also present in the *Juglans regia* (Delaviz, Mohammadi, Ghalamfarsa, Mohammadi, & Farhadi, 2017; Mollica et al., 2017).

Juglans regia is an edible plant belonging to the Juglandaceae family, its edible part known as kernel appears wrinkled and light in color. It is covered by a woody shell, called husk, which is green in color. There are ample anecdotal and scientific reports on the medicinal benefits of *Juglans regia* in the management of chronic diseases (Haque et al., 2003; Mateș et al., 2023; Rabiei et al., 2018), recently the nutraceutical benefits of *Juglans regia* walnut kernel has been also described in the management of diabetes mellitus (Mollica et al., 2017). In this current study, the effects of *Juglans regia* fresh fruits extract on normal and prostate cancer cell lines, and a rodent model of BPH was examined. The *in-vitro* antiproliferative and *in-vivo* ameliorative effects of the extract were assessed in order to delineate a complete biological profile, however more studies are due to determine its possible benefits in humans.

2. Methods and materials

2.1. Extract preparation

Juglans Regia immature fruits have been provided by a local vendor (Chieti, CH, Italy). They were picked two years ago in June and stored into a black glass airtight storage for 1 week before the use. *Juglans regia* fresh fruits (10 g) was used as is and triturated in blender to obtain a coarse powder and put in a closed vessel. A mixture of ethanol-water in a *ratio* 80:20 was added in the vessel. The *Juglans regia* fruits were macerated for 7 days shaking occasionally the vessel. Thus, the solid material was separated from the supernatant and pressed until the complete recovery of the solution. The total amount of supernatant was collected, filtered and finally evaporated by rotary evaporation (3.8 g). The obtained powder was stored at −20 °C for a maximum of two weeks.

2.2. Chromatographic analyses

First of all, approximately 5 mg of dried extract was dissolved in 1 mL of MeOH:H_2O 7:3 and filtered through 0.45 μm filters. The phytochemical profile was studied from a qualitative point of view to evaluate the main compounds present in the plant extract. An Agilent 1200 (Agilent Technologies, Santa Clara, CA, USA) equipped with an Agilent 6530B quadrupole-time-of-flight mass spectrometer (Q-TOF MS) was utilized. The column was a Luna Omega Polar C18 of 150 × 3.0 mm and 5 μm particle size (Phenomenex, Torrance, CA, USA) with a Polar C18 Security Guard cartridge of 4 × 3.0 mm. The mobile phases consisted of water + formic acid 0.1% v/v (eluent A) and acetonitrile + formic acid 0.1% (eluent B). The gradient elution was: 10%–25% B in 0–25 min, 25% B in 25–30 min and 25%–100% B in 30–35 min; in the end, eluent B was returned to 10% with a 7 min stabilization time. A flow rate of 0.4 mL min^{-1} was used. The Q-TOF MS was operated in the negative ion mode using an orthogonal ESI source. The parameters were: capillary voltage, 3500 V; nebulizer pressure of 45 psi; drying gas flow rate, 10 L/min; gas temperature, 325 °C; skimmer voltage, 60 V; fragmentor voltage, 140 V. Continuous internal calibration was performed during analyses with the use of signals at *m/z* 112.9855 and 1033.9881. The MS and Auto MS/MS modes (using collision energies of 10, 20 and 40 V) were set to acquire *m/z* values ranging between 50 and 1200, at a scan rate of 2 and 3 spectra per second, respectively. Agilent Mass Hunter Qualitative analysis software version B.06.00 was used for post-acquisition data processing. Once the phytochemical profile was established, the most abundant compounds were quantified (using the same HPLC program) using UV signals. The following analytical standards were used to quantify all the compounds of the same chemical family: gallic acid (280 nm), chlorogenic acid (320 nm), *p*-coumaric acid (320 nm), ellagic acid (250 nm) and quercetin (350 nm). Calibration curves were prepared in the range of 0.5–100 mg L^{-1}, plotting peak area versus concentration. R^2 was ≥ 0.999 for all the calibration graphs. For citric and isocitric acids, we used an analytical standard of citric acid and the quantification was performed in MS/MS mode using the 191 → 111 transition in the concentration range of 1–25 mg L^{-1}.

2.3. In vitro biochemical assays

2.3.1. Total quantification of phenolics and flavonoids

We determined the total phenolic and flavonoid content of the extract using the Folin-Ciocalteu and $AlCl_3$ assays, respectively as we had previously described (Zengin & Aktumsek, 2014). The results of these tests were reported in terms of gallic acid equivalents (mg GAE/g dry extract) and rutin equivalents (mg RE/g dry extract).

2.3.2. In vitro antioxidant and enzyme inhibition assays

We analyzed the extract for a range of antioxidant and enzyme inhibitory activities, including, cupric reducing antioxidant capacity (CUPRAC), DPPH and ABTS radical scavenging, metal chelating activity (MCA), ferric reducing antioxidant power (FRAP), phosphomolybdenum (PBD), and inhibition of amylase, tyrosinase, glucosidase, acetylcholinesterase (AChE), and butyrylcholinesterase (BChE). We employed the previously described methods to evaluate these activities (Uysal et al., 2017).

2.4. In vitro studies on human cells

2.4.1. Cell lines

DU145 human prostate carcinoma cell line (Catalogue no: HTB-81) was purchased from American Type Culture Collection (ATCC, Maryland, USA). PNT1A human post-pubertal prostate normal cell line (Catalogue no: 95012614) was purchased from European Collection of Authenticated Cell Cultures (ECACC, Wiltshire, England). DU145 cells were cultured in Dulbecco's Modified Eagle's Medium (DMEM – 4.5 g/L D-glucose, catalogue no: 41966029) (Gibco, Waltham, MA, USA) supplemented with 10% fetal bovine serum (FBS) (Biowest, Nuaillé, France), 100 units/mL penicillin and 100 μg/mL streptomycin (Gibco, Waltham, MA, USA). PNT1A cells were maintained in Roswell Park Memorial Institute 1640 Medium (RPMI 1640–4.5 g/L D-glucose, catalogue no: A1049101) (Gibco, Waltham, MA, USA) containing 10% FBS, 100 units/mL penicillin and, 100 μg/mL streptomycin. Both cell lines were cultured in a humidified atmosphere, in 5% CO_2 at 37 °C. Cells were cultured in a controlled manner in T75 flasks and passaged using trypsin-EDTA (0.25%), phenol red (Gibco, Waltham, MA, USA) when their confluency reached 80%. The main experiments were carried out when the cells were seen to have transitioned to their dynamic growth phase. Before the experiments, both viability control and cell counts were performed by hemocytometer using trypan blue dye exclusion method (Alafnan et al., 2023).

2.4.2. Real-time and label-free impedance-based cell proliferation assay

Anti-proliferative activities of *Juglans regia* extract against DU145 prostate carcinoma and PNT1A normal prostate cells were measured by iCELLigence real-time and label-free cell analysis system (Agilent Technologies (formerly ACEA Biosciences), San Diego, CA, USA) as we had previously described (Bender et al., 2023). With this technology, which determines the direct effects of experimental therapeutics on cells, the process is completed without any additional labeling or intervention (Bender et al., 2018; Lazarova et al., 2015). Accordingly, DU145 (1.0×10^4/well) and PNT1A (2.0×10^4/well) cells were seeded onto system-specific E-Plate L8 wells after a brief background measurement with growth medium. Plates were incubated in a laminar flow cabinet for 30 min to allow cells to migrate to the bottom of the well. Then they were placed in the iCELLigence instrument, and the study was started by programming to take measurements every 15 min for 96 h. Twenty-four hours after cell seeding, the experiment was paused and serial doses of *Juglans regia* extract (62.5–2000 μg/mL) were applied to

the cells in duplicate. Growth medium in which the extract was dissolved was used as negative control and Docetaxel (Taxotere®) was used as positive control. After all treatments, the experiment was continued again and was completed at the end of the 96th hour. Data analysis, visualization and IC50 calculations were performed in RTCA Data Analysis Software 1.0 (Agilent Technologies (formerly ACEA Biosciences), San Diego, CA, USA) (Bender et al., 2023).

2.5. In vivo studies

2.5.1. Animals

Adult male Wistar rats (Empire Breeders, Osun State, Nigeria) were used for this study. Rats were housed singly in metal cages located in temperature-controlled quarters (22–25 °C) with lights on at 7.00 a.m. daily. Animal diet was commercially sourced (TOP® feeds) standard rodent chow (29% protein, 13% fat, and 58% carbohydrate). Animals were allowed free access to food and water *ad libitum*. All experimental procedures were in accordance with the scientifically approved protocols of the Ladoke Akintola University of Technology and within international provisions for the Care and use of living animal [European Council Directive (EU2010/63)].

2.5.2. Experimental method

Experimental methods were performed in accordance with those reported in previous literature (Raafat et al. (2022), (Mollica et al., 2017) In brief, healthy adult rats weighing between 240 and 260 g were randomly assigned into five groups of 10 animals each (10 rats/group). The control group (group 1) received vehicle (olive oil, 1 mL/kg), while the BPH groups (groups 2–5) received a subcutaneous injection of testosterone enanthate at 3 mg/kg/day dissolved in vehicle to induce BPH as previously described. Following the induction of BPH, treatment was commenced with animals in group 1 and 2 being administered distilled water daily; while animals in the third and fourth groups were administered *Juglans regia* at 50 and 100 mg/kg body weight (doses of *Juglans regia* were selected taking cognizance of previous studies. Animals in the fifth group received a standard drug Finasteride at 5 mg/kg, body weight orally. Vehicle, Testosterone enantate, *Juglans regia* and finasteride were administered concurrently for 4 week. At the end of the experimental period animals were fasted overnight and blood taken via an intracadiac puncture for the estimation of testosterone levels, prostate specific antigen, luteinizing hormone and follicle stimulating hormone levels using standard protocols. Animals in all groups were euthanised by cervical dislocation following anaesthesia with chloroform. The prostate gland was either homogenised or excised, weighed, fixed in neutral buffered formolsaline and processed for general histological examination using hematoxylin and eosins and Van Geison's stain.

2.5.3. Assessment of body weight, relative prostatic weight and food intake

Body weight of animals in all groups were measured weekly using an electronic weighing scale (Mettler Toledo Type BD6000, Switzerland) while food consumption was assessed using a weighing balance daily as previously described Onaolapo et al. (Adejoke Yetunde Onaolapo & Onaolapo, 2018; O. J. Onaolapo et al., 2016). Percentage change in body weight or food intake was calculated for each animal using the equation below following which results for all animals were computed to find the statistical mean.

$$\frac{Final\ body\ weight\ or\ food\ intake - initial\ body\ weight\ or\ food\ intake}{Initial\ body\ weight\ or\ food\ intake}\ x\,100(\%)$$

The prostate gland was carefully dissected, weighed and washed in cold PBS following which it was blotted dry on a filter paper. The weight of the prostate and body weight were taken and relative prostatic weight calculated using the formula below

$$\frac{weight\ of\ prostate\ gland}{body\ weight\ oat\ sacrifice}\ (g)$$

2.5.4. Biochemical assays

2.5.4.1. Estimation of MDA content and antioxidant activity. Lipid peroxidation level was measured as malondialdehyde content as described previously (A. Onaolapo et al., 2019; Adejoke Yetunde Onaolapo, Sulaiman, Olofinnade, & Onaolapo, 2022). Change in color was measured using a spectrophotometer at 532 nm. Total antioxidant capacity was determined using commercially available assay kit. Total antioxidant capacity measures the quantity of free radicals scavenged by the test solution in any biological sample (O. J. Onaolapo et al., 2020). Total antioxidant capacity was based on the principle of the Trolox equivalent antioxidant capacity and assays were carried out as previously described (Olofinnade et al., 2020; Olofinnade, Onaolapo, Onaolapo, & Olowe, 2021).

2.5.4.2. Tumor necrosis factor-α, Interleukin-10 and interleukin-1β assays. Tumor necrosis factor-α and interleukin (IL)-10 were measured using enzyme-linked immunosorbent assay (ELISA) techniques with commercially available kits (Enzo Life Sciences Inc. NY, USA) designed to measure the 'total' (bound and unbound) amount of the respective cytokinesas previously described (Adejoke Y Onaolapo, Ojo, & Onaolapo, 2023). Interleukin1 β level were assayed using enzyme-linked immunosorbent assay (ELISA) techniques with commercially available kits (Enzo Life Sciences Inc. NY, USA) following the instructions of the manufacturers.

2.5.4.3. Testosterone, luteinizing and follicle stimulating hormone assay. Total testosterone level was measured using commercially available radioimmunoassay kits (Tianjin Medical & Bioengineering Co., Ltd.), as previously described (A. Onaolapo, Oladipo, & Onaolapo, 2018; O. J. Onaolapo et al., 2016). The levels of follicle stimulating hormone (FSH), and luteinizing hormone (LH), were measured using enzyme linked immunosorbent assay (ELISA) kit (ABNOVA).

2.6. Histopathological study

Formalin-fixed samples of the prostate gland were embedded in paraffin and sectioned (5 μm thickness). Sections of the prostatic tissue were then dewaxed and rehydrated following which they were mounted on slides and stained with hematoxylin–eosin (H&E) for general histological study while assessment of the connective tissue of the prostate gland was done using the Van Gieson's stain. Sections of the prostate gland were examined microscopically using a Sellon-Olympus trinocular microscope (XSZ-107E, Ningbo Beilun Fangyuan Photoelectric Instrument Co., Ltd. Zhejiang, China) with a digital camera (Canon Powershot 2500, Chaoyang, Beijing, China), and photomicrographs taken. Histopathological changes were assessed by a technician that was blinded to the groupings.

2.7. Statistical analysis

Data were analyzed using Chris Rorden's ANOVA for windows (MRIcro Analyze, version 0.98, Columbia, SC, USA), by One-way analysis of variance (ANOVA) and post-hoc test (Tukey HSD) for group comparisons. Results were expressed as mean ± S.E.M. and $p < 0.05$ was taken as the accepted level of significant difference from control (*) or BPH control (&).

3. Results and discussion

3.1. Characterization of phytochemicals by HPLC-ESI-Q-TOF-MS

Thirty-eight compounds have been identified or tentatively characterized in the extract of *Juglans regia* (Table 1). The characterization has been done using accurate mass data, ion source fragmentation, MS/MS fragmentation patterns and bibliographic search, as well as analytical standards of citric acid, gallic acid, chlorogenic acid, neochlorogenic acid, coumaric acid, catechin, myricetin, ellagic acid, and quercetin. Table 1 shows the assigned identification, retention time, experimental $[M-H]^-$, molecular formula, calculated mass error (ppm) and fragment ions for each compound. The base peak chromatogram is shown in Fig. 1. Compounds **1** and **5** show $[M-H]^-$ at *m/z* 191 and the same fragmentation pattern with base peak at *m/z* 111.Using an analytical standard, **5** was unequivocally identified as citric acid, so compound **1** was assigned as isocitric acid. Compound **2** has been identified as ascorbic acid based on its molecular formula and the fragmentation pattern reported in literature. Compounds **3**, **8**, **11**, **15** presented $[M-H]^-$ at *m/z* 783 and fragment ions at *m/z* 481, 301, 275 and 249. These compounds were identified as bis-hexahydroxydiphenoyl-hexoside, as previously reported in scientific bibliography (Bresciani et al., 2015). Compound **4** was characterized as malic acid based on molecular formula, exact mass and fragment ions at *m/z* 115 and 71. Compound **7** was identified as gallic acid using an analytical standard. Many derivatives of gallic acid were characterized based on the neutral losses observed during the fragmentation and the fragment ions at *m/z* 169 and 125 (characteristic of gallic acid). Compound **6** was characterized as galloyl-*O*-hexoside due to the neutral loss of 162 Da (hexoside moiety) to yield gallic acid at *m/z* 169. Compounds **26**, **31** and **37** present a similar fragmentation pattern compared to compound **6**, thus they were tentatively characterized as galloyl-*O*-hexosidederivatives. Compound **13** was identified as galloyl-hexahydroxydiphenoyl-hexoside comparing the fragmentation pattern to the data in literature (Bresciani et al., 2015) and considering the fragment ion at *m/z* 169 (gallic acid). Compound **14** was characterized as methyl gallate due to its molecular formula, $[M-H]^-$ at *m/z* 183 and fragment ions at *m/z* 168 and 124 showing a neutral loss of 15 Da corresponding to a methyl moiety. Compound **24**, $[M-H]^-$ at *m/z* 197 and fragment ions at *m/z* 169 and 124, was characterized as ethyl gallate, showing a neutral loss of 28 Da ($-CH_2CH_2-$). Compound **27** was tentatively characterized as a gallic acid derivative. Compound **9** was characterized as hydroxymethylglutaric acid due to its molecular formula and its fragmentation pattern previously reported in literature (Tahir et al., 2012). Compound **10** was characterized as dimethylcitric acid because of its molecular formula and observed $[M-H^-]$ at *m/z* 219. Compounds **12** and **19** were characterized as neochlorogenic acid and chlorogenic acid using analytical standards. Compounds **17** and **25** have been identified as coumaric acid isomers based on their molecular formula and both showing the typical fragmentation pattern *m/z*163→119 (compared with an analytical standard). Compounds **16** and **22** were characterized as 3-*p*-coumaroylquinic acid and 4-*p*-coumaroylquinic acid, respectively, based on their molecular formula, observed $[M-H]^-$ at *m/z* 337 and base peaks at *m/z* 163 and 173, respectively, according to the hierarchical scheme reported by Clifford et al. (Clifford, Johnston, Knight, & Kuhnert, 2003). Compounds **18** and **21** both displayed $[M-H]^-$ at *m/z* 289 and fragment ions at *m/z* 245, 205, 203 and 179. Based on the different retention time, they were characterized respectively as catechin and (epi)catechin by using an analytical standard of catechin. Compound **29** was identified as taxifolin based on the $[M-H]^-$ at *m/z* 303, the molecular formula and the characteristic fragmentation (Hashim et al., 2013). Compounds **28** and **35** (*m/z* 435 → 303) were identified as taxifolin-*O*-pentoside isomers due to the neutral loss of 132 Da (pentoside moiety). Compound **30,** with $[M-H]^-$ at *m/z* 463 and fragment ions at *m/z* 317 and 271, was characterized as myricetin-*O*-deoxyhexoside. The fragmentation *m/z*463→317 displayed a neutral loss of 146 Da corresponding to the deoxyhexoside moiety. Compound **33** was identified as ellagic acid using an analytical standard. Compound **41** with $[M-H]^-$ at *m/z* 301 and fragment ions at *m/z* 179 and 151, has been identified as quercetin by comparison with an analytical standard. Moreover, several quercetin glycosides have been found in this extract; compounds **32** and **34** were identified as quercetin-*O*--hexoside isomers, compounds **38** and **39** as quercetin-*O*-pentoside isomers, and compound **40** as quercetin-*O*-deoxyhexoside.

3.1.1. Quantification of the main compounds

A heat map was prepared to determine the relative contribution of each compound to the whole extract (Fig. 2). For each compound, the peak area in MS mode was determined using the precursor ion $[M-H]^-$; then, the relative contribution (%) of each compound regarding the sum of the areas of all compounds was calculated. The compounds present in higher concentrations are characterized by a darker colour in the heat map. The most abundant compounds were malic acid (**4**), hydroxymethylglutaric acid (**9**), coumaroylquinic acids (**16** and **22**), gallic acid derivatives (**24** and **26**) and caffeoylquinic acids (**12** and **19**). High levels of malic acid were previously reported, as well as high levels of caffeoylquinic acids and coumaric acid derivatives (Santos et al., (Vieira et al., 2019; Zhao, Jiang, Liu, & Li, 2014; Żurek, Pycia, Pawłowska, Potocki, & Kapusta, 2023). Quantification was performed for the main phenolic acids and flavonoids responsible for the bioactivity. The results are shown in Table 2. The most abundant compounds were gallic acid and derivatives (6.6 mg g^{-1}), caffeoylquinic acids (2.91 mg g^{-1}) and coumaric acid derivatives (4.87 mg g^{-1}). The abundance of caffeoylquinic acids and coumaric acid derivatives agrees with previous works on *Juglans regia* (Santos et al., 2013; Vieira et al., 2019; Zhao et al., 2014; Żurek et al., 2023).

3.2. Total bioactive compounds, antioxidant, and enzyme inhibitory effects

Phenolic compounds play a crucial role as key constituents among plant secondary metabolites, and their levels provide initial insights into the potential of plant extracts (Matsumura, Kitabatake, Kayano, & Ito, 2023). In this study, we evaluated the total phenolic and flavonoid contents in the extract using colorimetric methods as a primary assessment. The results showed that the total phenolic content was 41.68 mg GAE/g, while the total flavonoid content was 3.96 mg RE/g (Table 3). Notably, flavonoids accounted for approximately 10% of the phenolic in the tested extracts, as supported by HPLC-MS/MS analysis, which revealed their presence as a minor group within the phenolic composition. In the existing literature, researchers have reported varying levels of total bioactive compounds in *Juglans regia* extracts which can be attributed to geographical and climatic factors such as altitude, soil composition, annual rainfall, and sunlight exposure. The antioxidant properties of the tested extracts were assessed using various chemical methods, including free radical scavenging assays (ABTS and DPPH), reducing power assays (CUPRAC and FRAP), metal chelating assays, and phosphomolybdenum assays (Table 3). Among these, the ABTS and DPPH assays are widely used to measure the antioxidant capacity, reflecting the ability of antioxidant compounds to neutralize free radicals. In our study, the tested extract demonstrated significant radical scavenging abilities in both assays, with results of 76.86 mg TE/g and 45.73 mg TE/g, respectively. Furthermore, the reducing ability of the extracts was evaluated using the CUPRAC and FRAP assays, which assess the electron-donation capacity of antioxidants. The extract demonstrated notable reducing ability in the assays, with values of 206.93 mg TE/g (CUPRAC) and 139.56 mg TE/g (FRAP). Metal chelation ability is an important mechanism associated with inhibiting the production of hydroxyl radicals in the Fenton reaction. The tested extract exhibited significant metal chelation ability, with a value of 20.00 mg EDTAE/g. Additionally, the extract displayed activity in the phosphomolybdenum assay, which involves the transformation of Mo (VI) to Mo (V) by antioxidant compounds under acidic conditions. The tested extract

Table 1
Characterization of the compounds found in *Juglans regia* fresh fruits extract.

No.	t_R (min)	Observed [M-H]$^-$	Molecular formula	Error (ppm)	Fragment ions	Assigned identification
1	1.904	191.0199	$C_6H_8O_7$	−0.91	173.0073 129.0183 **111.0081** 87.0085 85.0291	Isocitric acid
2	2.028	175.0247	$C_6H_8O_6$	0.69	**115.0032**	Ascorbic acid
3	2.151	783.0686	$C_{34}H_{24}O_{22}$	−0.23	481.0580 **300.9992** 275.0190 249.0399	Bis-HHDP-hexoside
4	2.274	133.0142	$C_4H_6O_5$	0.13	**115.0031** 71.0141	Malic acid
5	2.520	191.0203	$C_6H_8O_7$	−2.45	173.0086 129.0188 **111.0081** 87.0085 85.0293	Citric acid
6	2.767	331.0671	$C_{13}H_{16}O_{10}$	−0.19	**271.0455** 211.0253 169.0140 125.0239	Galloyl-*O*-hexoside
7	3.260	169.0144	$C_7H_6O_5$	−0.8	**125.0241**	Gallic acid
8	3.691	783.0685	$C_{34}H_{24}O_{22}$	−0.48	481.0622 **300.9987** 275.0191 249.0391	Bis-HHDP-hexoside
9	3.937	161.0461	$C_6H_{10}O_5$	−2.99	143.0350 **99.0450** 71.0143	Hydroxymethylglutaric acid
10	4.615	219.0512	$C_8H_{12}O_7$	−0.65	**111.0089** 87.0091 67.0191 57.0357	Dimethylcitric acid
11	4.677	783.0687	$C_{34}H_{24}O_{22}$	−0.87	481.0630 **300.9987** 275.0197 249.0397	Bis-HHDP-hexoside
12	5.416	353.0880	$C_{16}H_{18}O_9$	−0.14	**191.0557** 179.0343 135.0450	Neochlorogenic acid
13	5.909	633.0731	$C_{27}H_{22}O_{18}$	0.41	**300.9993** 275.0191 169.0310	Galloyl-HHDP-hexoside
14	6.463	183.0298	$C_8H_8O_5$	0.45	**168.0057** 124.0157	Methyl gallate
15	7.018	783.0687	$C_{34}H_{24}O_{22}$	−0.57	481.0685 **300.9992** 275.0198 249.0392	Bis-HHDP-hexoside
16	7.818	337.0929	$C_{16}H_{18}O_8$	−0.01	**163.0395** 119.0499	3-*p*-coumaroylquinic acid
17	7.880	163.0398	$C_9H_8O_3$	1.62	**119.0512**	Coumaric acid isomer
18	9.051	289.0718	$C_{15}H_{14}O_6$	−0.45	**245.0807** 205.0519 203.0709 179.0346 125.0249	Catechin
19	9.174	353.0879	$C_{16}H_{18}O_9$	−0.9	**191.0556** 179.0329 173.0445 135.0467	Chlorogenic acid
20	9.543	339.1087	$C_{16}H_{20}O_8$	−0.31	179.0559 **159.0450** 119.0343 89.0244	Unknown
21	12.358	289.0717	$C_{15}H_{14}O_6$	1.38	**245.0818** 205.0496 203.0720 179.0353 125.0250	(epi)catechin
22	12.482	337.0930	$C_{16}H_{18}O_8$	−0.33	**173.0453** 93.0341	4-*p*-coumaroylquinic acid
23	12.913	331.0460	$C_{16}H_{12}O_8$	−1.74	**271.0247** 227.0350	Unknown

(*continued on next page*)

Table 1 (*continued*)

No.	t_R (min)	Observed [M-H]$^-$	Molecular formula	Error (ppm)	Fragment ions	Assigned identification
24	14.268	197.0456	$C_9H_{10}O_5$	−0.3	169.0140 **124.0162**	Ethyl gallate
25	16.714	163.0400	$C_9H_8O_3$	0.65	**119.0499**	*p*-Coumaric acid
26	19.188	491.1191	$C_{23}H_{24}O_{12}$	0.85	331.0668 **271.0454** 211.0244 169.0135 125.0242 124.0163	Galloyl-*O*-hexoside derivative
27	19.558	475.1243	$C_{23}H_{24}O_{11}$	0.66	313.0550 271.0444 211.0243 **169.0139** 151.0016 124.0177 123.0082	Gallic acid derivative
28	19.681	435.0932	$C_{20}H_{20}O_{11}$	0.57	**303.0495** 285.0390 151.0040 125.0227	Taxifolin-*O*-pentoside
29	19.989	303.0512	$C_{15}H_{12}O_7$	−0.35	**285.0396** 177.0189 175.0395 125.0239	Taxifolin
30	20.653	463.0882	$C_{21}H_{20}O_{12}$	−0.96	317.0279 **316.0224** 287.0154 271.0221	Myricetin-*O*-deoxyhexoside
31	21.022	507.1138	$C_{23}H_{24}O_{13}$	1.2	331.0673 **271.0442** 211.0259 169.0097 125.0242	Galloyl-*O*-hexoside derivative
32	21.454	463.0878	$C_{21}H_{20}O_{12}$	0.96	301.0334 **300.0268** 271.0224 255.0311 178.9988 151.0027	Quercetin-*O*-hexoside
33	21.515	300.9992	$C_{14}H_6O_8$	−0.73	257.0077 **229.0139**	Ellagic acid
34	21.823	463.0884	$C_{21}H_{20}O_{12}$	0.2	**301.0334** 178.9988 151.0098	Quercetin-*O*-hexoside
35	22.008	435.0930	$C_{20}H_{20}O_{11}$	0.61	**303.0501** 285.0408 151.0031 125.0244	Taxifolin-*O*-pentoside
36	22.809	229.0146	$C_{12}H_6O_5$	−1.45	**201.0191** 173.0239 145.0280 117.0339	Unknown
37	23.834	489.1038	$C_{23}H_{22}O_{12}$	0.27	331.0660 313.0565 **271.0457** 211.0246 169.0141 125.0232 124.0158	Galloyl-*O*-hexoside derivative
38	24.019	433.0773	$C_{20}H_{18}O_{11}$	0.56	301.0310 **300.0278** 271.0238 255.0234 151.0023	Quercetin-*O*-pentoside
39	24.635	433.0777	$C_{20}H_{18}O_{11}$	0.46	**301.0345** 300.0277 271.0230 255.0278 178.9998 151.0019	Quercetin-*O*-pentoside
40	25.212	447.0929	$C_{21}H_{20}O_{11}$	0.92	**301.0341** 271.0257 255.0292 151.0031	Quercetin-*O*-deoxyhexoside
41	35.920	301.0352	$C_{15}H_{10}O_7$	0.5	178.9966 **151.0038**	Quercetin

HHDP = hexahydroxydiphenoyl.

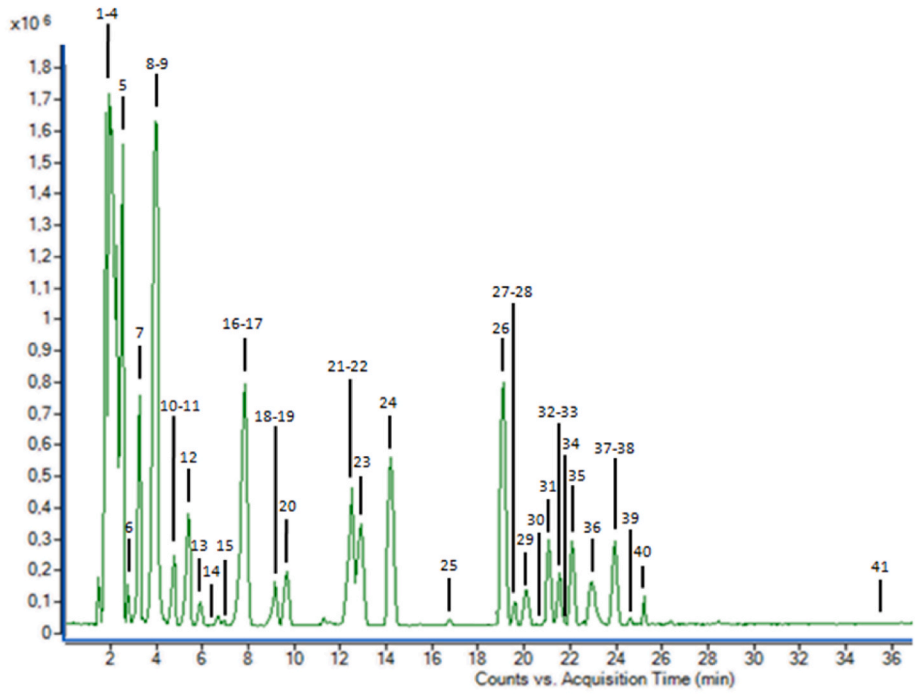

Fig. 1. HPLC-ESI-Q-TOF-MS base peak chromatogram of *Juglans regia* fresh fruits extract.

exhibited activity in this assay, with a result of 2.29 mmol TE/g. Tables 1–3 report the compounds that can be attributed to the observed antioxidant abilities. Notably, gallic, chlorogenic, and ellagic acid are potential contributors to the antioxidant effects observed. The hydroxyl groups positioned at the meta and para positions within the phenolic ring of gallic acid actively participate in radical quenching and electron donation, as observed in reducing power assays. Ellagic acid, as studied by Priyadarsini, Khopde, Kumar, and Mohan (2002), exhibited significant abilities in DPPH and ABTS radical scavenging assays. Furthermore, the research by Xu, Hu, and Liu (2012) indicated that chlorogenic acid and its derivatives showed noteworthy actions in radical scavenging (ABTS and DPPH) and reducing power (FRAP) assays. The authors also suggested that the number and position of hydroxyl groups can influence the antioxidant properties of these compounds. Enzyme inhibition plays a crucial role in managing significant global health challenges, including diabetes mellitus, Alzheimer's disease, and obesity, thus we explored the inhibitory effects of the tested extract on various enzymes, namely cholinesterases, amylase, glucosidase, and tyrosinase. In the context of Alzheimer's disease management, cholinesterases *e.g.* AChE and BChE, are of primary importance. Table 2 provides an overview of the inhibitory potentials of the tested extract on both cholinesterases, with values of 5.69 mg GALAE/g for AChE and 1.92 mg GALAE/g for BChE. Amylase and glucosidase are pivotal enzymes involved in the breakdown of carbohydrates. The reversible inhibition of these enzymes is essential for regulating blood glucose levels in individuals with diabetes. In our study, we observed inhibitory effects of the tested extract on these antidiabetic enzymes, with values of 0.39 mmol ACAE/g for amylase and 0.90 mmol ACAE/g for glucosidase. Tyrosinase a primary enzyme responsible for melanin synthesis, it plays a crucial role in managing hyperpigmentation issues. The tested extract demonstrated inhibition of tyrosinase, with a result of 92.29 mg KAE/g extract. The observed inhibitory effects on enzymes can be attributed to specific compounds present in the tested extract. For instance, chlorogenic acid has been documented as a significant inhibitor of cholinesterases by Oboh, Agunloye, Akinyemi, Ademiluyi, and Adefegha (2013). Additionally, Zheng et al. (2020) reported the inhibitory effects of chlorogenic acid against amylase. In another study by Oh et al. (2021), ellagic acid demonstrated potent inhibitory potential against AChE, exhibiting a low IC_{50} value. Furthermore, Yin et al. (2018) reported superior inhibitory effects of ellagic acid and its derivatives from Mongolian oak cups on amylase and glucosidase activities.

3.3. Cellular activities

In this study, time and dose-dependent anti-proliferative analyzes were performed to observe the effects of *Juglans regia* extract on human prostate cancer and normal cells. In this context, we selected the DU145 prostate carcinoma cell line, which is one of the most widely used cell model in prostate cancer research. We also used healthy prostatic cells, PNT1A, which is a useful tool in prostate research. The test method used is critical in cell viability assays, especially in natural extract-based studies. Considering that extracts are a huge phytochemical library, a direct analysis method that will not interfere with these compounds is of great importance. The xCELLigence systems provide consistent quality control and data through real-time and label-free cell analysis technology, unlike traditional endpoint analyzes (Bender & Atalay, 2018; Picot et al., 2017). The system uses specially designed microtiter E-Plates which contain ~80% gold microelectrodes embedded in the bottom of each well. The impedance measurement is performed by applying a low electric current to the plates, which flows between the microelectrodes through an ionic-cell culture medium solution. The cells seeded in E-Plate wells acting as electrical insulators when adhered to microelectrodes. The adherent cells affect the impedance signal which is automatically measured according to a user-defined frequency. Thus, the biological status information of the cell such as viability, cell index, and morphology, is obtained by non-invasive and real-time manner (Bender & Atalay, 2018, 2021; Bird & Kirstein, 2009). In this study, the iCELLigence model of the xCELLigence ecosystem was used. 24 h after seeding DU145 or PNT1A cells onto the system, they were treated with six serial doses (62.5–2000 μg/mL) of *Juglans regia* or positive control

Peak	Compound	Relative contribution (%)
1	Isocitric acid	2.93
2	Ascorbic acid	3.03
3	Bis-HHDP-hexoside	0.16
4	Malic acid	19.48
5	Citric acid	3.06
6	Galloyl-*O*-hexoside	0.38
7	Gallic acid	3.45
8	Bis-HHDP-hexoside	0.25
9	Hydroxymethylglutaric acid	14.33
10	Dimethylcitric acid	1.74
11	Bis-HHDP-hexoside	0.39
12	Neochlorogenic acid	2.68
13	Galloyl-HHDP-hexoside	0.69
14	Methyl gallate	0.15
15	Bis-HHDP-hexoside	0.35
16	3-*p*-Coumaroylquinic acid	7.41
17	Coumaric acid isomer	0.43
18	Catechin	1.03
19	Chlorogenic acid	1.50
20	Unknown	1.54
21	(epi)catechin	0.29
22	4-*p*-Coumaroylquinic acid	4.52
23	Unknown	3.56
24	Ethyl gallate	4.86
25	*p*-Coumaric acid	0.24
26	Galloyl-*O*-hexoside derivative	6.47
27	Gallic acid derivative	0.52
28	Taxifolin-*O*-pentoside	0.77
29	Taxifolin	1.42
30	Myricetin-*O*-deoxyhexoside	0.11
31	Galloyl-*O*-hexoside derivative	2.04
32	Quercetin-*O*-hexoside	0.33
33	Ellagic acid	1.72
34	Quercetin-*O*-hexoside	0.06
35	Taxifolin-*O*-pentoside	2.08
36	Unknown	2.36
37	Galloyl-*O*-hexoside derivative	2.26
38	Quercetin-*O*-pentoside	0.15
39	Quercetin-*O*-pentoside	0.23
40	Quercetin-*O*-deoxyhexoside	0.69
41	Quercetin	0.32

HHDP=hexahydroxydiphenoyl.

Fig. 2. Heat map obtained by HPLC-Q-TOF-MS analysis of *Juglans regia* fresh fruits extract. HHDP = hexahydroxydiphenoyl.

drug Docetaxel and activity was monitored for 72 h. Viability measurements taken every 15 min were recorded during the total experiment period of 96 h and are shown in Fig. 3. Also, the viability rates for each dose every 24 h after treatment are given in Table 4 for DU145 and in Table 5 for PNT1A. It was observed that 2000 μg/mL *Juglans regia* was cytotoxic on both cells from the first time it was applied, and even had comparable growth inhibition with Docetaxel. This situation was also confirmed by the decreasing viability rates with increasing time. A similar situation was observed at 1000 μg/mL, although not as potently as 2000 μg/mL. However, a 2-fold confidence interval was observed at

Table 2
Concentration of phytochemicals found in *Juglans regia* fruit extract.Values (mg/g DE) is the mean ± SD of three parallel measurements.

N°	Assigned identification	mg/gDE
1	Isocitric acid	0.84 ± 0.06
5	Citric acid	1.3 ± 0.1
6	Galloyl-*O*-hexoside	0.31 ± 0.02
7	Gallic acid	2.2 ± 0.2
12	Neochlorogenic acid	1.9 ± 0.1
13	Galloyl-HHDP-Hex	0.39 ± 0.03
16 + 17	3-*p*-CoQA + coumaric acid isomer	2.9 ± 0.2
19	Chlorogenic acid	1.01 ± 0.07
22	4-*p*-CoQA	1.5 ± 0.1
24	Ethyl gallate	1.27 ± 0.09
25	*p*-Coumaric acid	0.47 ± 0.03
26	Galloyl-*O*-Hex derivative	1.9 ± 0.1
31	Galloyl-*O*-Hex derivative	0.39 ± 0.03
33	Ellagic acid	1.4 ± 0.1
35	Taxifolin-*O*-Pen	0.22 ± 0.02
37	Galloyl-*O*-Hex derivative	0.53 ± 0.04
39	Quercetin-*O*-Pen	0.17 ± 0.01
40	Quercetin-*O*-dHex	0.27 ± 0.02
Total		**19.0 ± 0.4**

HHDP = hexahydroxydiphenoyl; CoQA = coumaroylquinic acid; Hex = hexoside; Pen = pentoside; dHex = deoxyhexoside; DE = dried extract.

Table 3
Total bioactive compounds, antioxidant, and enzyme inhibitory effects of the tested extract.

Parameters	Results
Total bioactive compounds	
Total phenolic content (mg GAE/g)	41.68 ± 0.25
Total flavonoid content (mg RE/g)	3.96 ± 0.05
Antioxidant effects	
DPPH (mg TE/g)	45.73 ± 0.11
ABTS (mg TE/g)	76.86 ± 0.10
CUPRAC (mg TE/g)	206.93 ± 13.47
FRAP (mg TE/g	139.56 ± 2.94
Metal chelating (mg EDTAE/g)	20.00 ± 0.20
PBD (mmol TE/g)	2.29 ± 0.02
Enzyme inhibitory effects	
AChE (mg GALAE/g)	5.69 ± 0.05
BChE (mg GALAE/g)	1.92 ± 0.18
Tyrosinase (mg KAE/g)	92.29 ± 0.53
α-Amylase (mmol ACAE/g)	0.39 ± 0.03
α-Gluosidase (mmol ACAE/g)	0.90 ± 0.01

Values are reported as mean ± SD of three parallel measurements. GAE: Gallic acid equivalent; RE: Rutin equivalent; TE: Trolox equivalent; EDTAE: EDTA equivalent; GALAE: Galanthamine equivalent; KAE: Kojic acid equivalent; ACAE: Acarbose equivalent; PBD: Phosphomolybdenum assay.

these doses for healthy cells at 72nd-hours. Other doses ranged from 62.5 μg/mL to 500 μg/mL, a time- and dose-dependent increased growth inhibition was observed compared to control cells. At all doses in this range, DU145 cells were more inhibited by *Juglans regia* compared to PNT1A cells at the 72 nd h of treatment. IC50 values were analyzed using cell index data at 96th hours and calculated as 263.4 μg/mL for DU145 cells and >500 μg/mL for PNT1A cells with R^2 values greater than 0.99, respectively. Based on the IC50 values, it was observed that *Juglans regia* showed time- and dose-dependent anti-proliferative activity against prostate cancer cells, as well as having a minimum 2-fold safer profile for healthy prostatic cells.

3.4. *In vivo studies*

3.4.1. *Effect of Juglans regia on body weight, food intake, prostatic weight and prostate specific antigen levels*

Fig. 4 shows the effect of *Juglans regia* extract on physiological

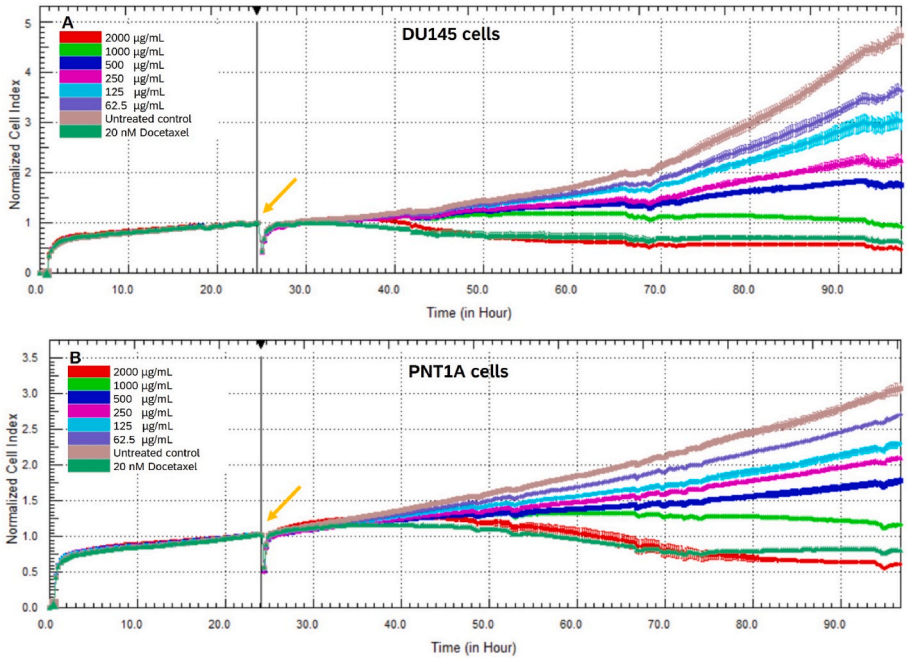

Fig. 3. Real-time, label-free, and high-throughput monitoring of *Juglans regia* fresh fruits extract effects on DU145 prostate carcinoma and PNT1A normal prostate human cells with iCELLigence system. The yellow arrow indicates the treatment point (~24th hour). **A.** DU145 cells **B.** PNT1A cells. (For interpretation of the references to color in this figure legend, the reader is referred to the Web version of this article.)

Table 4
DU145 cell viability rates (%) at 24-, 48-, and 72- hours treatments with *Juglans regia* fresh fruits extract or Docetaxel (Min %Control).

Time point	Cell Viability (% ± SEM)							
	Control	Juglans regia (µg/mL)						Docetaxel
		2000	1000	500	250	125	62.5	20 nM
24 h	98.23 ± 0.00	55.21 ± 0.01	82.46 ± 0.00	88.05 ± 0.01	87.40 ± 0.03	93.64 ± 0.01	94.17 ± 0.00	55.64 ± 0.05
48 h	97.69 ± 0.00	23.81 ± 0.00	48.30 ± 0.00	61.81 ± 0.02	67.59 ± 0.02	79.20 ± 0.02	86.88 ± 0.02	29.53 ± 0.02
72 h	97.34 ± 0.01	9.90 ± 0.01	19.71 ± 0.00	37.21 ± 0.02	47.76 ± 0.02	64.21 ± 0.04	76.90 ± 0.02	13.24 ± 0.01

Table 5
PNT1A cell viability rates (%) at 24-, 48-, and 72- hours treatments with *Juglans regia* fresh fruits extract or Docetaxel (Min %Control).

Time point	Cell Viability (% ± SEM)							
	Control	Juglans regia (µg/mL)						Docetaxel
		2000	1000	500	250	125	62.5	20 nM
24 h	98.44 ± 0.02	78.14 ± 0.02	83.79 ± 0.01	83.81 ± 0.01	87.31 ± 0.01	89.90 ± 0.01	94.19 ± 0.00	71.97 ± 0.00
48 h	98.44 ± 0.02	34.32 ± 0.04	57.63 ± 0.01	66.57 ± 0.01	74.53 ± 0.00	79.15 ± 0.02	89.74 ± 0.01	34.67 ± 0.00
72 h	98.44 ± 0.02	18.43 ± 0.00	37.54 ± 0.00	57.22 ± 0.02	67.75 ± 0.00	73.82 ± 0.01	86.66 ± 0.00	25.65 ± 0.00

parameters. Body weight increased across all groups throughout the four week experimental period (Fig. 4A). A gradual increase in weight was observed in the groups administered *Juglans regia* and finasteride however, in the BPH control group weight increase was steep. Percentage change in body weight (Fig. 4B) revealed a significant increase in the BPH control group (47.9%) and with *Juglans regia* at 100 mg/kg (32.6%), while a decrease in body weight was observed with finasteride (25.6%) compared to control (28.5%). Compared to BPH control percentage change in body weight decreased with *Juglans regia* at 50 (29.4%), 100 (32.6%) mg/kg and with finasteride (25.6%).

Fig. 4C shows the effect of *Juglans regia* extract on weekly changes in food intake and Fig. 4D indicates percentage change in food intake throughout the experimental period. Food intake increased across all groups except the finasteride group which showed no significant weekly change in food intake throughout the experimental period. Percentage change in food intake revealed a significant increase in food intake with BPH control group (33.7%) and a decrease with finasteride (8.9%) compared to control (21.5%). Compared to BPH control however, percentage change in food intake decreased with *Juglans regia* at 50 (18.9%) and 100 (19.6%) mg/kg and with finasteride (8.9%)

Fig. 4E shows the effect of *Juglans regia* extract on relative prostatic weight and Fig. 4F expresses prostate specific antigen levels. Relative prostatic weight increased significantly with BPH control, *Juglans regia* (50 and 100) and finasteride compared to control. Compared to BPH control, relative prostatic weight decreased with *Juglans regia* (at 50 and 100) and with finasteride. Prostate specific antigen levels increased significantly with BPH control, *Juglans regia* (50 and 100) and finasteride compared to control. Compared to BPH control prostate specific antigen levels decreased with *Juglans regia* (at 50 and 100) and with finasteride.

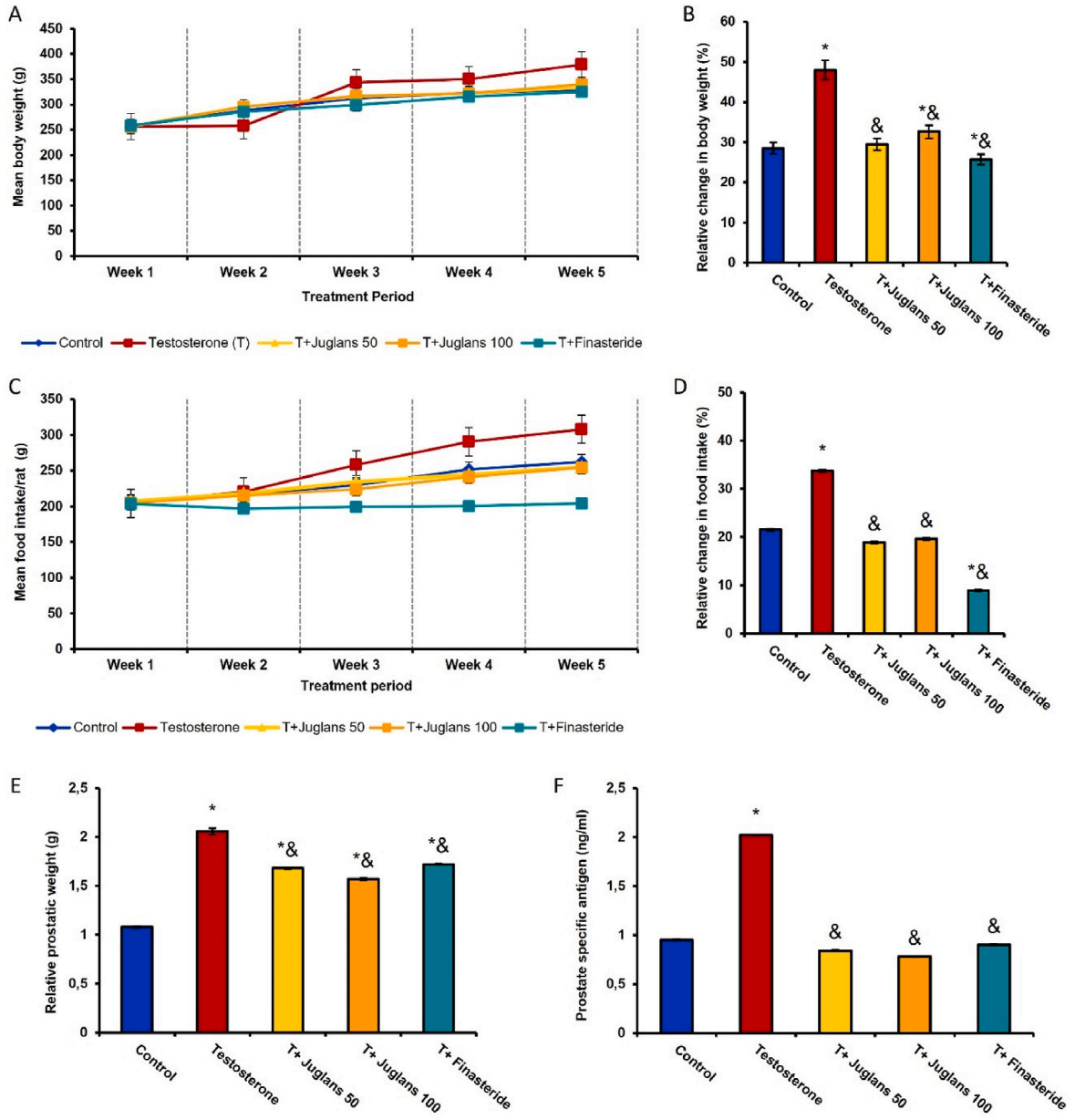

Fig. 4. Effect of *Juglans regia* fresh fruits extract on weekly body weight (A), percentage change in weight (B), mean weekly food intake (C), percentage change in food intake (D), relative prostate weight (E), prostate specific antigen levels (F) in testosterone treated male rats. Each bar represents Mean ± S.E.M, number of rats per treatment group = 10. T: Testosterone, $p < 0.05$ was taken as the accepted level of significant difference from control (*) or BPH control (&).

3.4.2. Effect of Juglans regia on testosterone levels, superoxide dismutase activity, lipid peroxidation and total antioxidant capacity

Fig. 5 shows the effect of *Juglans regia* extract on testosterone levels (Fig. 5A) and superoxide dismutase activity (Fig. 5B). Testosterone levels increased significantly with BPH control, finasteride and decreased with *Juglans regia* at 100 mg/kg body weight compared to control. Compared to BPH control, testosterone levels decreased significantly with *Juglans regia* (at 50 and 100) and increased with finasteride.

Superoxide dismutase activity decreased significantly with BPH control, finasteride and increased with *Juglans regia* (50 and 100) compared to control. Compared to BPH control, superoxide dismutase activity increased with *Juglans regia* (at 50 and 100).

Fig. 5C shows the effect of *Juglans regia* extract on lipid peroxidation levels and Fig. 5D demonstrates total antioxidant capacity. Lipid peroxidation levels increased significantly with BPH control, *Juglans regia* (50 & 100) and finasteride compared to control. Compared to BPH control lipid peroxidation levels decreased significantly with *Juglans regia* (at 50 and 100) and increased finasteride. Total antioxidant capacity decreased significantly with BPH control and finasteride and increased with *Juglans regia* (50 and 100) compared to control. Compared to BPH control total antioxidant capacity increased with *Juglans regia* (at 50 and 100) and finasteride.

3.4.3. Effect of Juglans regia on tumour necrosis factor-α, Interleukin-10, interleukin 1β and gonadotrophic hormone level

Fig. 5E shows the effect of *Juglans regia* extract on Tumour necrosis factor-α and Fig. 5F expresses interleukin-10 levels. Tumour necrosis factor-α increased significantly with BPH control, *Juglans regia* (50 & 100) and finasteride compared to control. Compared to BPH control, there was a significant decrease in tumour necrosis factor-α level with *Juglans regia* at 50 and 100.I nterleukin-10 decreased significantly with BPH control, *Juglans regia* (50 and 100) and finasteride compared to control. Compared to BPH control, interleukin-10 levels increased with

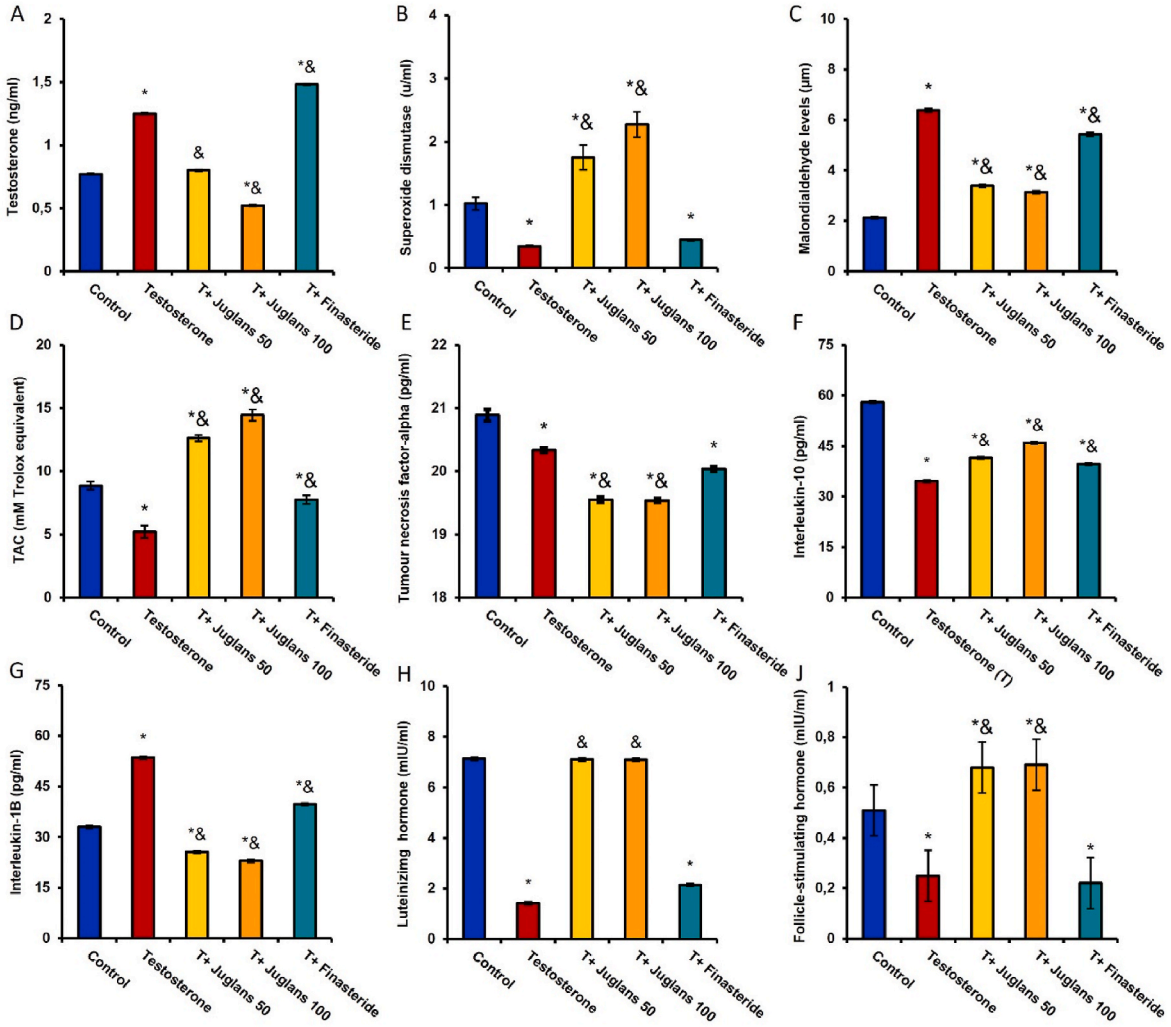

Fig. 5. Effect of *Juglans regia* fresh fruits extract on testosterone levels (A), super oxide dismutase activity (B), malondialdehyde levels (C), total antioxidant capacity (D), tumor necrosis factor-αlpha (E), interleukin-10 (F), Interleukin1β (G), luteinizing hormone (H) and, follicle-stimulating hormone (J) in testosterone treated male rats. Each bar represents Mean ± S.E.M, number of rats per treatment group = 10. T: Testosterone, $p < 0.05$ was taken as the accepted level of significant difference from control (*) or BPH control (&).

Juglans regia (at 50 and 100) and finasteride.

Fig. 5G shows the effect of *Juglans regia* extract on interleukin 1β and Fig. 5H and J indicate gonadotrophic hormone levels including luteinizing and follicle stimulating hormone, respectively. Interleukin 1β increased significantly with BPH control, finasteride and decreased with *Juglans regia* (50 & 100) compared to control. Compared to BPH control, there was a significant decrease in interleukin 1βlevel with *Juglans regia* (at 50 and 100) and finasteride. Luteinizing hormone (LH) levels decreased significantly with BPH control, and finasteride compared to control. Compared to BPH control, LH levels increased with *Juglans regia* at 50 and 100. Follicle stimulating hormone (FSH) levels decreased significantly with BPH control, and finasteride and increased with *Juglans regia* at 50 and 100 mg/kg body weight compared to control. Compared to BPH control, FSH levels increased with *Juglans regia* (at 50 and 100).

3.4.4. *Effect of Juglans regia on prostate histology and prostatic epithelial hyperplasia*

Histological assessment of the prostate gland of rats in control group revealed (at low magnification) branching ducts of glandular tissue, surrounded by stroma (made up largely of smooth muscle fibres and connective tissue) (Fig. 6). The epithelial tissue surrounding the individual glands is bilayered comprising of a luminal layer of flattened simple columnar cells and a basal layer of cuboidal cells with basophilic nuclei. In groups of rats with testosterone-induced BPH there was significant hyperplasia of the epithelial tissue with pale staining pyknotic nuclei. In the groups administered *Juglans regia* (at 50 and 100 mg/kg body weight) or finasteride amelioration of the changes observed with testosterone induced BPH was observed. Examination of slides stained with Van Geison's stain revealed normal rat prostate histology with minimal smooth muscle tissue (staining yellow) and collagen tissue (staining red) in the control group. In the BPH groups there is an increase in smooth muscle tissue staining and less collagen staining. Papillary projections into the gland are also observed. In groups administered *Juglans regia* at 50 mg/kg and significant redness of the gland signifying an increase in collagen staining in the 100 mg/kg body weight *Juglans* group. In the group administered finasteride there is a significant yellowing of the glandular tissue and intervening stroma.

In this study, the administration of testosterone for the induction of BPH was associated with increased body weight, food intake, and increased relative weight of the prostate gland. While this observation supports studies reporting the administration of testosterone associated with these changes (Alrabadi et al., 2020; Elbaz, Amin, Kamel, Ibrahim, & Helmy, 2020; A. Onaolapo et al., 2018; O. J. Onaolapo et al., 2016; Raafat et al., 2022) it also supports its use as an animal model of BPH (Elbaz et al., 2020; Jeon et al., 2017; Raafat et al., 2022). Weight gain

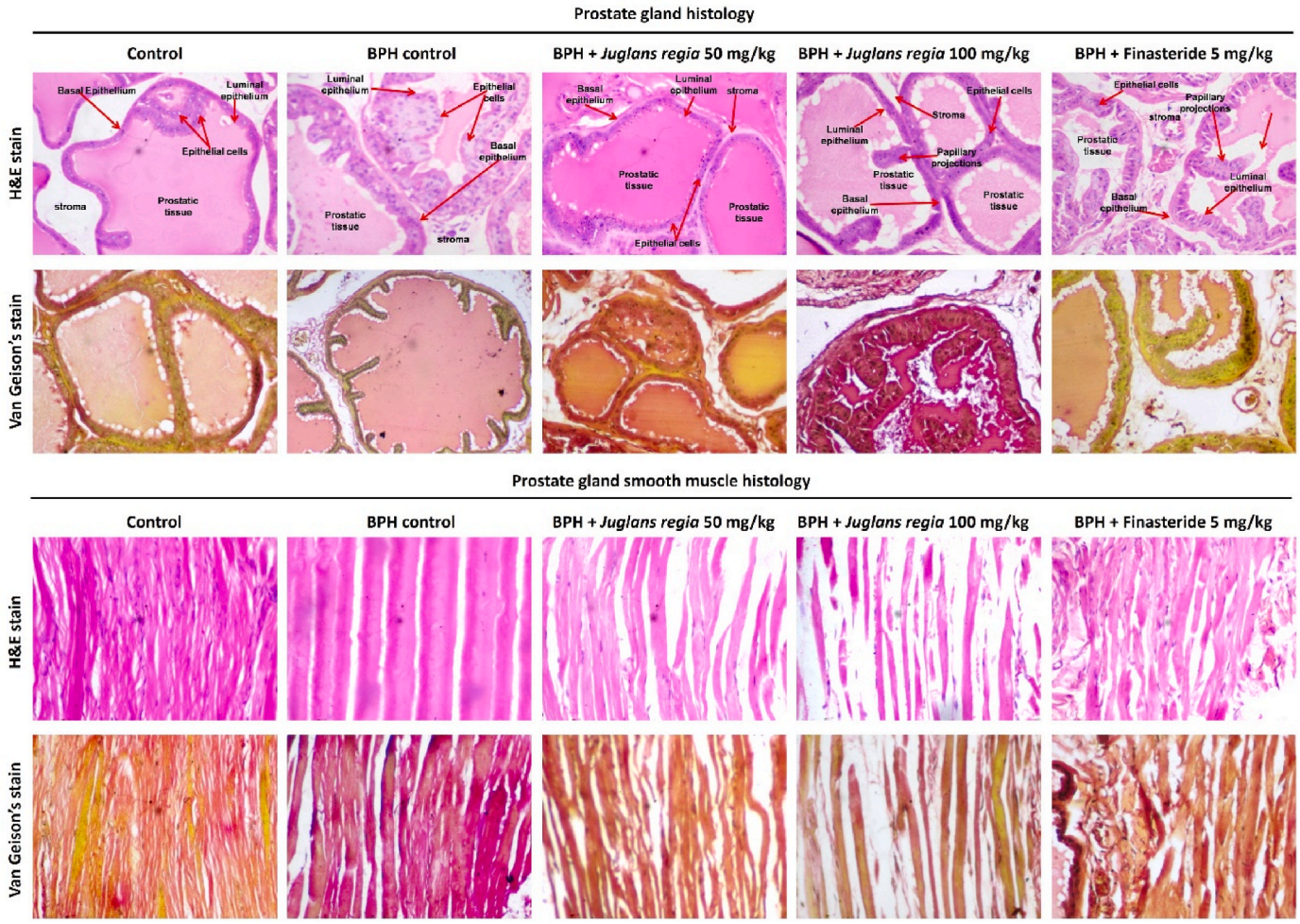

Fig. 6. Effect of *Juglans regia* fresh fruits extract on prostate gland histology and prostate gland smooth muscle histology with H&E staining and Van Geison's stain. Representative photomicrographs of control, benign prostatic hyperplasia (BPH) control, BPH and *Juglans regia* at 50 mg/kg, BPH and *Juglans regia* at 100 mg/kg and, BPH and Finasteride at 5 mg/kg. Magnification, 560 × for prostate gland histology. Magnification, 160 × for prostate gland smooth muscle histology.

observed in this study can be attributed to the anabolic effects of testosterone which mediate an increase in food intake and increase skeletal muscle mass.

The relationship between body weight and BPH have been examined extensively, and there is ample scientific evidence associating increased body weight, obesity and dysmetabolism with the development of benign prostatic hyperplasia (J. K. Kim, Lee, Han, & Han, 2021; Parikesit, Mochtar, Umbas, & Hamid, 2016; Parsons, Sarma, McVary, & Wei, 2013; Xue et al., 2020). Obesity has also been reported to worsen BPH symptoms through mechanisms that include increasing intra-abdominal pressure, alteration of endocrine status, increased inflammation and oxidative stress and increased sympathetic nervous activity. In this study also an increase in the weight of the prostate gland as well as increased PSA levels were observed. Generally, the enlargement of the prostate gland measured as increased prostate weight is considered a very important marker of the development and progression of BPH. In this study, testosterone-induced BPH was associated with an increase in the weight of the prostate gland according to others (Jeon et al., 2017; Yang, Yuan, Xiong, Yin, & Ruan, 2014), The administration of *Juglans regia* extract in this study reversed testosterone-induced increase in body weight, food intake, prostatic weight and prostate specific antigen levels. The effects of *Juglans regia* on body weight has been examined (Ashraf, Arfeen, Amjad, & Ahmed, 2020; Rabiei et al., 2018) with reports associating the administration of *Juglans regia* with the lowering of body weight in humans and experimental animals. The ability of *Juglans regia* extract to mitigate changes in the prostate gland has also been reported. Davis et al. (2012) and H. Kim, Yokoyama, and Davis (2014) reported that the administration of *Juglans regia* in a mouse model of prostatic cancer was associated with reduced prostatic weight suggesting that *Juglans regia* had the ability to act on the prostate gland and reverse important mechanisms that result in disease. Prostate-specific antigen is a serine protease enzyme that is produced by the columnar epithelium of prostatic tissue and has become useful as a fairly reliable screening tool in prostate disease. In this study, *Juglans regia* was associated with a reversal of testosterone-induced increase in PSA levels. While this could occur as a result of a decrease in the size of the prostate gland and reduced epithelial cell hyperplasia observed on histology.

In this test, induction of BPH was associated with an increase in testosterone levels, which was also observed in the group administered finasteride, however in the groups administered *Juglans regia,* a reversal of testosterone induced increase in prostatic testosterone levels was observed. Although it has been reported that an inverse relationship exists between serum testosterone levels and prostate volume in aging men, studies in laboratory animals have also drawn some association between levels of testosterone and the development of a BPH in experimental animals, however more recent studies in humans have reported that high testosterone and increased PSA levels are significantly associated with increased prostatic volume among persons with BPH. The use of testosterone to induce BPH resulted in an increase in testosterone and PSA levels, this would suggest that both increase oxidative stress and their association must be also deranged. The administration of

Juglans regia extract and not finasteride was associated with a reversal of testosterone-induced changes, according with the ability of *Juglans regia* extract to decrease testosterone levels in diabetes mellitus induced testicular dysfunction.

Studies have shown that oxidative stress and increased inflammation are important factors in the development, progression and management of BPH (Quintero-García et al., 2018; Shabani et al., 2021). In this study the BPH control animals showed increased lipid peroxidation reduced superoxide dismutase activity and increased total antioxidant capacity consistent with increased oxidative stress. They also exhibited increase in the level of proinflammatory markers TNF-α and IL-1β, while a decrease in the levels of anti-inflammatory markers (IL-10) was observed consistent with the results of studies (Jeon et al., 2017; Quintero-García et al., 2018; Shabani et al., 2021). Testosterone induced increase in serum testosterone levels can also be implicated in the increased oxidative stress observed in this study. A report on cardiac myocytes described that testosterone increased reactive oxygen species production and oxidative stress through genomic and non-genomic signaling of the androgen receptor (Cruz-Topete, Dominic, & Stokes, 2020). Here, the administration of *Juglans regia* extract was associated with a reversal of testosterone induced changes in oxidative stress or inflammatory markers (Fizeșan et al., 2021; Rusu, Fizesan, et al., 2020; Rusu, Georgiu, et al., 2020). The antioxidant and anti-inflammatory effects of *Juglans regia* extract has been attributed to its high phenolic content. The results of our *in vitro* tests corroborate the antioxidant properties of *Juglans* observed in the *in vivo* assays. The antioxidant and anti-inflammatory properties of *Juglans regia* extract in this study exceed those observed with finasteride suggesting its potential application in the development of novel therapies for BPH progresses.

Histological examination of the smooth muscle tissue of the stroma revealed normal smooth muscle histology in the control group; this is evidenced by strands of non-striated muscle tissue with central nuclei. In the BPH group hyperplasia of smooth muscle tissue is observed with loss of central nuclei in keeping with smooth muscle hyperplasia. In the groups administered *Juglans regia* or finasteride there was a reversal of the BPH changes, although in the finasteride group disorganization of the smooth muscle tissue was also observed. Van Geison staining revealed yellow staining of the muscle tissue in the control group, this is in keeping with normal smooth muscle histology. In the BPH group however pinkish staining of muscle tissue is observed, which is in keeping with increased fibrous tissue. In the groups administered *Juglans regia* or finasteride there was a reversal of the changes observed with BPH.

It is generally accepted that BPH arises from the enlargement of the gland's glandular and stromal tissue that surround the prostatic urethra. In this study we observe changes that support results of previous studies in which *Juglans regia* extract was associated with a reversal of the changes observed with BPH control (Spaccarotella et al., 2008). The ameliorative effects of *Juglans regia* fresh fruits extract could be attributed to its antioxidant and anti-inflammatory properties associated with the high content of bioactive compounds.

4. Conclusion

Many studies have been documented on the strong relationship between BPH and prostate cancer risk (Dai, Fang, Ma, & Xianyu, 2016; Ørsted & Bojesen, 2013). Both of them affect the prostate gland and share common symptoms. Proposed mechanisms of action of *Juglans regia* extract in inhibiting prostate cancer in rats include induction of apoptosis, modulation of cell signaling pathways, and anti-inflammatory effects. Our study revealed that the most abundant compounds were gallic acid and derivatives (6.6 mg g^{-1}), caffeoylquinic acids (2.91 mg g^{-1}) and coumaric acid derivatives (4.87 mg g^{-1}). Gallic acid reduces the progression of prostate cancer by inhibition of HDACs (Jang, Ko, & Choi, 2020). Gallic acid is a potent apoptotic inducer on various cancer types (Liu, Li, Yu, & Niu, 2012; Wang et al., 2016). We think that the strong bioactive contents in *Juglans regia* fresh fruits extract is effective in inhibiting the hallmarks of cancer. Several animal studies have investigated the effects of *Juglans regia* extract or components on prostate cancer. These studies often use mice or rats that have been implanted with prostate cancer cells. Other mammals that have been known to develop prostate cancer include canine models, non-human primates, lions and, transgenic models as reported by the NCI Mouse Models of Human Cancers Consortium (Ittmann et al., 2013). However, induced prostate cancer is possible in rodents such as rats. Further studies along the line of our present work may be possible using canine models. Regarding the clinical trials, although these mechanisms have been proposed based on animal models, further research is due to extrapolate these findings on humans.

Overall, in this work a complete panel of *in vivo* and *in vitro* biological activities has been investigated for *Juglans regia* fresh fruits extract. This exerts a cell protecting function *in vivo* on human prostatic cancer cell line together with a strong antioxidant and enzyme inhibitory activity. Taken together, the extract tested can serve as valuable natural source of enzyme inhibitors against global health problems. Our study, which determined the complete anti-proliferative profile of *Juglans regia* fresh fruits extract against prostate cancer and normal cells, suggests its potential as a promising agent for prostate cancer management.

Fundings

This work has been funded *by the European Union -NextGenerationEU under the Italian Ministry of University and Research (MUR) National Innovation Ecosystem* grant *ECS00000041 -VITALITY -CUP **[D73C22000840006]***.

CRediT authorship contribution statement

Azzurra Stefanucci: Writing – review & editing, Writing – original draft, Project administration, Conceptualization. **Lorenza Marinaccio:** Validation, Methodology, Investigation. **Eulogio J. Llorent-Martínez:** Data curation, Formal analysis, Methodology, Visualization, Methodology, Formal analysis, Data curation. **Gokhan Zengin:** Visualization, Formal analysis, Data curation. **Onur Bender:** Visualization, Methodology, Data curation. **Rumeysa Dogan:** Visualization, Methodology, Data curation. **Arzu Atalay:** Visualization, Methodology, Data curation. **Omotayo Adegbite:** Resources. **Foluso O. Ojo:** Resources. **Adejoke Y. Onaolapo:** Visualization, Formal analysis, Data curation. **Olakunle J. Onaolapo:** Visualization, Formal analysis, Data curation. **Adriano Mollica:** Supervision, Resources.

Declaration of competing interest

The authors declare that they have no known competing financial interests or personal relationships that could have appeared to influence the work reported in this paper.

Data availability

Data will be made available on request.

Acknowledgements

Technical and human support provided by CICT of Universidad de Jaén (UJA, MINECO, Junta de Andalucía, FEDER) is gratefully acknowledged. We are grateful to PON MUR Ricerca Innovazione 2014-2020 for PhD funds of L.M.

References

Ak, G., Zengin, G., Ceylan, R., Fawzi Mahomoodally, M., Jugreet, S., Mollica, A., et al. (2021). Chemical composition and biological activities of essential oils from

Calendula officinalis L. flowers and leaves. *Flavour and Fragrance Journal, 36*(5), 554–563.
Alafnan, A., Dogan, R., Bender, O., Celik, I., Mollica, A., Malik, J., et al. (2023). Beta Elemene induces cytotoxic effects in FLT3 ITD-mutated acute myeloid leukemia by modulating apoptosis. *European Review for Medical and Pharmacological Sciences, 27*(8).
Alrabadi, N., Al-Rabadi, G. J., Maraqa, R., Sarayrah, H., Alzoubi, K. H., Alqudah, M., et al. (2020). Androgen effect on body weight and behaviour of male and female rats: Novel insight on the clinical value. *Andrologia, 52*(10), Article e13730.
Ashraf, S., Arfeen, A., Amjad, S., & Ahmed, Z. (2020). Effect of walnut (Juglans Regia) consumption on hyperlipidemic adults. *Food Science and Technology, 41*, 432–438.
Bender, O., & Atalay, A. (2018). Evaluation of anti-proliferative and cytotoxic effects of chlorogenic acid on breast cancer cell lines by real-time, label-free and high-throughput screening. *Marmara Pharmaceutical Journal, 22*(2).
Bender, O., & Atalay, A. (2021). Polyphenol chlorogenic acid, antioxidant profile, and breast cancer. In *Cancer* (pp. 311–321). Elsevier.
Bender, O., Celik, I., Dogan, R., Atalay, A., Shoman, M. E., Ali, T. F., et al. (2023). Vanillin-based indolin-2-one derivative bearing a pyridyl moiety as a promising anti-breast cancer agent via anti-estrogenic activity. *ACS Omega, 8*(7), 6968–6981.
Bender, O., Llorent-Martínez, E. J., Zengin, G., Mollica, A., Ceylan, R., Molina-Garcia, L., et al. (2018). Integration of *in vitro* and *in silico* perspectives to explain chemical characterization, biological potential and anticancer effects of *Hypericum salsugineum*: A pharmacologically active source for functional drug formulations. *PLoS One, 13*(6), Article e0197815.
Bird, C., & Kirstein, S. (2009). *Real-time, label-free monitoring of cellular invasion and migration with the xCELLigence system*. New York: Nature Publishing Group US.
Bresciani, L., Calani, L., Cossu, M., Mena, P., Sayegh, M., Ray, S., et al. (2015). Poly) phenolic characterization of three food supplements containing 36 different fruits, vegetables and berries. *PharmaNutrition, 3*(2), 11–19.
Choi, H.-M., Jung, Y., Park, J., Kim, H.-L., Youn, D.-H., Kang, J., et al. (2016). Cinnamomi cortex (*Cinnamomum verum*) suppresses testosterone-induced benign prostatic hyperplasia by regulating 5α-reductase. *Scientific Reports, 6*(1), Article 31906.
Clifford, M. N., Johnston, K. L., Knight, S., & Kuhnert, N. (2003). Hierarchical scheme for LC-MS^n identification of chlorogenic acids. *Journal of Agricultural and Food Chemistry, 51*(10), 2900–2911.
Cruz-Topete, D., Dominic, P., & Stokes, K. Y. (2020). Uncovering sex-specific mechanisms of action of testosterone and redox balance. *Redox Biology, 31*, Article 101490.
Csikós, E., Horváth, A., Ács, K., Papp, N., Balázs, V. L., Dolenc, M. S., et al. (2021). Treatment of benign prostatic hyperplasia by natural drugs. *Molecules, 26*(23), 7141.
Dai, X., Fang, X., Ma, Y., & Xianyu, J. (2016). Benign prostatic hyperplasia and the risk of prostate cancer and bladder cancer: A meta-analysis of observational studies. *Medicine, 95*(18), e3493.
Davis, P. A., Vasu, V. T., Gohil, K., Kim, H., Khan, I. H., Cross, C. E., et al. (2012). A high-fat diet containing whole walnuts (*Juglans regia*) reduces tumour size and growth along with plasma insulin-like growth factor 1 in the transgenic adenocarcinoma of the mouse prostate model. *British Journal of Nutrition, 108*(10), 1764–1772.
Delaviz, H., Mohammadi, J., Ghalamfarsa, G., Mohammadi, B., & Farhadi, N. (2017). A review study on phytochemistry and pharmacology applications of Juglans regia plant. *Pharmacognosy Reviews, 11*(22), 145.
Elbaz, E. M., Amin, H. A. A., Kamel, A. S., Ibrahim, S. M., & Helmy, H. S. (2020). Immunomodulatory effect of diallyl sulfide on experimentally-induced benign prostate hyperplasia via the suppression of CD4+ T/IL-17 and TGF-β1/ERK pathways. *Inflammopharmacology, 28*, 1407–1420.
Fagelman, E., & Lowe, F. C. (2002). Herbal medications in the treatment of benign prostatic hyperplasia (BPH). *Urologic Clinics, 29*(1), 23–29.
Fizeşan, I., Rusu, M. E., Georgiu, C., Pop, A., Ştefan, M.-G., Muntean, D.-M., et al. (2021). Antitussive, antioxidant, and anti-inflammatory effects of a walnut (*Juglans regia* L.) septum extract rich in bioactive compounds. *Antioxidants, 10*(1), 119.
Haque, R., Bin-Hafeez, B., Parvez, S., Pandey, S., Sayeed, I., Ali, M., et al. (2003). Aqueous extract of walnut (*Juglans regia* L.) protects mice against cyclophosphamideinduced biochemical toxicity. *Human & Experimental Toxicology, 22*(9), 473–480.
Hashim, S. N., Schwarz, L. J., Boysen, R. I., Yang, Y., Danylec, B., & Hearn, M. T. (2013). Rapid solid-phase extraction and analysis of resveratrol and other polyphenols in red wine. *Journal of Chromatography A, 1313*, 284–290.
Ittmann, M., Huang, J., Radaelli, E., Martin, P., Signoretti, S., Sullivan, R., et al. (2013). Animal models of human prostate cancer: The consensus report of the New York meeting of the mouse models of human cancers Consortium prostate pathology committee. *Cancer Research, 73*(9), 2718–2736.
Jang, Y.-G., Ko, E.-B., & Choi, K.-C. (2020). Gallic acid, a phenolic acid, hinders the progression of prostate cancer by inhibition of histone deacetylase 1 and 2 expression. *The Journal of nutritional biochemistry, 84*, Article 108444.
Jeon, W.-Y., Kim, O. S., Seo, C.-S., Jin, S. E., Kim, J., Shin, H.-K., et al. (2017). Inhibitory effects of Ponciri Fructus on testosterone-induced benign prostatic hyperplasia in rats. *BMC Complementary and Alternative Medicine, 17*(1), 1–10.
Kim, J. K., Lee, Y. G., Han, K., & Han, J. H. (2021). Obesity, metabolic health, and urological disorders in adults: A nationwide population-based study. *Scientific Reports, 11*(1), 8687.
Kim, H., Yokoyama, W., & Davis, P. A. (2014). TRAMP prostate tumor growth is slowed by walnut diets through altered IGF-1 levels, energy pathways, and cholesterol metabolism. *Journal of Medicinal Food, 17*(12), 1281–1286.
Lazarova, I., Zengin, G., Bender, O., Zheleva-Dimitrova, D., Uysal, S., Ceylan, R., et al. (2015). A comparative study of Bulgarian and Turkish *Asphodeline lutea* root extracts: HPLC–UV profiles, enzyme inhibitory potentials and anti-proliferative activities against MCF-7 and MCF-10a cell lines. *Journal of Functional Foods, 15*, 254–263.
Liu, Z., Li, D., Yu, L., & Niu, F. (2012). Gallic acid as a cancer-selective agent induces apoptosis in pancreatic cancer cells. *Chemotherapy, 58*(3), 185–194.
Mateș, L., Rusu, M. E., & Popa, D.-S. (2023). Phytochemicals and biological activities of walnut septum: A systematic review. *Antioxidants, 12*(3), 604.
Matsumura, Y., Kitabatake, M., Kayano, S.-i., & Ito, T. (2023). Dietary phenolic compounds: Their health benefits and association with the gut microbiota. *Antioxidants, 12*(4), 880.
Mollica, A., Zengin, G., Locatelli, M., Stefanucci, A., Macedonio, G., Bellagamba, G., et al. (2017). An assessment of the nutraceutical potential of *Juglans regia* L. leaf powder in diabetic rats. *Food and Chemical Toxicology, 107*, 554–564.
Oboh, G., Agunloye, O. M., Akinyemi, A. J., Ademiluyi, A. O., & Adefegha, S. A. (2013). Comparative study on the inhibitory effect of caffeic and chlorogenic acids on key enzymes linked to Alzheimer's disease and some pro-oxidant induced oxidative stress in rats' brain-*in vitro*. *Neurochemical Research, 38*, 413–419.
Oh, J. M., Jang, H.-J., Kang, M.-G., Song, S., Kim, D.-Y., Kim, J. H., et al. (2021). Acetylcholinesterase and monoamine oxidase-B inhibitory activities by ellagic acid derivatives isolated from *Castanopsis cuspidata* var. sieboldii. *Scientific Reports, 11*(1), Article 13953.
Olofinnade, A. T., Onaolapo, A. Y., Onaolapo, O. J., & Olowe, O. A. (2021). Hazelnut modulates neurobehaviour and ameliorates ageing-induced oxidative stress, and caspase-3-mediated apoptosis in mice. *Current Aging Science, 14*(2), 154–162.
Olofinnade, A. T., Onaolapo, A. Y., Onaolapo, O. J., Olowe, O. A., Mollica, A., Zengin, G., et al. (2020). *Corylus avellana* L. modulates neurobehaviour and brain chemistry following high-fat diet. *Frontiers in Bioscience-Landmark, 26*(3), 537–551.
Onaolapo, A., Ayeni, O., Ogundeji, M., Ajao, A., Onaolapo, O., & Owolabi, A. (2019). Subchronic ketamine alters behaviour, metabolic indices and brain morphology in adolescent rats: Involvement of oxidative stress, glutamate toxicity and caspase-3-mediated apoptosis. *Journal of Chemical Neuroanatomy, 96*, 22–33.
Onaolapo, O. J., Jegede, O. R., Adegoke, O., Ayinde, M. O., Akeredolu, O. M., & Onaolapo, A. Y. (2020). Dietary zinc supplement militates against ketamine-induced behaviours by age-dependent modulation of oxidative stress and acetylcholinesterase activity in mice. *Pharmacological Reports, 72*, 55–66.
Onaolapo, A. Y., Ojo, F. O., & Onaolapo, O. J. (2023). Biflavonoid quercetin protects against cyclophosphamide–induced organ toxicities via modulation of inflammatory cytokines, brain neurotransmitters, and astrocyte immunoreactivity. *Food and Chemical Toxicology*, Article 113879.
Onaolapo, A., Oladipo, B., & Onaolapo, O. (2018). Cyclophosphamide-induced male subfertility in mice: An assessment of the potential benefits of Maca supplement. *Andrologia, 50*(3), Article e12911.
Onaolapo, A. Y., & Onaolapo, O. J. (2018). Nevirapine mitigates monosodium glutamate induced neurotoxicity and oxidative stress changes in prepubertal mice. *Annals of Medical Research, 25*(4), 518–524.
Onaolapo, O. J., Onaolapo, A. Y., Omololu, T. A., Oludimu, A. T., Segun-Busari, T., & Omoleke, T. (2016). Exogenous testosterone, aging, and changes in behavioral response of gonadally intact male mice. *Journal of Experimental Neuroscience, 10*. JEN. S39042.
Onaolapo, A. Y., Sulaiman, H., Olofinnade, A. T., & Onaolapo, O. J. (2022). Antidepressant-like potential of silymarin and silymarin-sertraline combination in mice: Highlighting effects on behaviour, oxidative stress, and neuroinflammation. *World Journal of Pharmacology, 11*(3), 27–47.
Ørsted, D. D., & Bojesen, S. E. (2013). The link between benign prostatic hyperplasia and prostate cancer. *Nature Reviews Urology, 10*(1), 49–54.
Parikesit, D., Mochtar, C. A., Umbas, R., & Hamid, A. R. A. H. (2016). The impact of obesity towards prostate diseases. *Prostate international, 4*(1), 1–6.
Parsons, J. K., Sarma, A. V., McVary, K., & Wei, J. T. (2013). Obesity and benign prostatic hyperplasia: Clinical connections, emerging etiological paradigms and future directions. *The Journal of Urology, 189*(1), S102–S106.
Picot, M. C. N., Bender, O., Atalay, A., Zengin, G., Loffredo, L., Hadji-Minaglou, F., et al. (2017). Multiple pharmacological targets, cytotoxicity, and phytochemical profile of *Aphloia theiformis* (Vahl.) Benn. *Biomedicine & Pharmacotherapy, 89*, 342–350.
Pieretti, S., Saviano, A., Mollica, A., Stefanucci, A., Aloisi, A. M., & Nicoletti, M. (2022). Calceolarioside A, a phenylpropanoid glycoside from *Calceolaria* spp., displays antinociceptive and anti-inflammatory properties. *Molecules, 27*(7), 2183.
Priyadarsini, K. I., Khopde, S. M., Kumar, S. S., & Mohan, H. (2002). Free radical studies of ellagic acid, a natural phenolic antioxidant. *Journal of Agricultural and Food Chemistry, 50*(7), 2200–2206.
Quintero-García, M., Delgado-González, E., Sánchez-Tusie, A., Vázquez, M., Aceves, C., & Anguiano, B. (2018). Iodine prevents the increase of testosterone-induced oxidative stress in a model of rat prostatic hyperplasia. *Free Radical Biology and Medicine, 115*, 298–308.
Raafat, M., Kamel, A. A., Shehata, A. H., Ahmed, A.-S. F., Bayoumi, A. M., Moussa, R. A., et al. (2022). Aescin protects against experimental benign prostatic hyperplasia and preserves prostate histomorphology in rats via suppression of inflammatory cytokines and cox-2. *Pharmaceuticals, 15*(2), 130.
Rabiei, K., Ebrahimzadeh, M. A., Saeedi, M., Bahar, A., Akha, O., & Kashi, Z. (2018). Effects of a hydroalcoholic extract of *Juglans regia* (walnut) leaves on blood glucose and major cardiovascular risk factors in type 2 diabetic patients: A double-blind, placebo-controlled clinical trial. *BMC Complementary and Alternative Medicine, 18*(1), 1–7.
Rusu, M. E., Fizesan, I., Pop, A., Mocan, A., Gheldiu, A.-M., Babota, M., et al. (2020). Walnut (*Juglans regia* L.) septum: Assessment of bioactive molecules and *in vitro* biological effects. *Molecules, 25*(9), 2187.

Rusu, M. E., Georgiu, C., Pop, A., Mocan, A., Kiss, B., Vostinaru, O., et al. (2020). Antioxidant effects of walnut (*Juglans regia* L.) kernel and walnut septum extract in a D-galactose-induced aging model and in naturally aged rats. *Antioxidants, 9*(5), 424.

Santos, A., Barros, L., Calhelha, R. C., Dueñas, M., Carvalho, A. M., Santos-Buelga, C., et al. (2013). Leaves and decoction of Juglans regia L.: Different performances regarding bioactive compounds and in vitro antioxidant and antitumor effects. *Industrial Crops and Products, 51*, 430–436.

Shabani, E., Kalantari, H., Kalantar, M., Goudarzi, M., Mansouri, E., & Kalantar, H. (2021). Berberine ameliorates testosterone-induced benign prostate hyperplasia in rats. *BMC Complementary Medicine and Therapies, 21*(1), 1–10.

Spaccarotella, K. J., Kris-Etherton, P. M., Stone, W. L., Bagshaw, D. M., Fishell, V. K., West, S. G., et al. (2008). The effect of walnut intake on factors related to prostate and vascular health in older men. *Nutrition Journal, 7*(1), 1–10.

Tahir, N. I., Shaari, K., Abas, F., Parveez, G. K. A., Ishak, Z., & Ramli, U. S. (2012). Characterization of apigenin and luteolin derivatives from oil palm (Elaeis guineensis Jacq.) leaf using LC–ESI-MS/MS. *Journal of Agricultural and Food Chemistry, 60*(45), 11201–11210.

Uysal, S., Zengin, G., Locatelli, M., Bahadori, M. B., Mocan, A., Bellagamba, G., et al. (2017). Cytotoxic and enzyme inhibitory potential of two *Potentilla* species (*P. speciosa* L. and *P. reptans* Willd.) and their chemical composition. *Frontiers in Pharmacology, 8*, 290.

Vieira, V., Pereira, C., Pires, T. C., Calhelha, R. C., Alves, M. J., Ferreira, O., et al. (2019). Phenolic profile, antioxidant and antibacterial properties of *Juglans regia* L.(walnut) leaves from the Northeast of Portugal. *Industrial Crops and Products, 134*, 347–355.

Wang, R., Ma, L., Weng, D., Yao, J., Liu, X., & Jin, F. (2016). Gallic acid induces apoptosis and enhances the anticancer effects of cisplatin in human small cell lung cancer H446 cell line via the ROS-dependent mitochondrial apoptotic pathway. *Oncology Reports, 35*(5), 3075–3083.

Xue, B., Wu, S., Sharkey, C., Tabatabaei, S., Wu, C.-L., Tao, Z., et al. (2020). Obesity-associated inflammation induces androgenic to estrogenic switch in the prostate gland. *Prostate Cancer and Prostatic Diseases, 23*(3), 465–474.

Xu, J.-G., Hu, Q.-P., & Liu, Y. (2012). Antioxidant and DNA-protective activities of chlorogenic acid isomers. *Journal of Agricultural and Food Chemistry, 60*(46), 11625–11630.

Yang, X., Yuan, L., Xiong, C., Yin, C., & Ruan, J. (2014). Abacopteris penangiana exerts testosterone-induced benign prostatic hyperplasia protective effect through regulating inflammatory responses, reducing oxidative stress and anti-proliferative. *Journal of Ethnopharmacology, 157*, 105–113.

Yin, P., Yang, L., Xue, Q., Yu, M., Yao, F., Sun, L., et al. (2018). Identification and inhibitory activities of ellagic acid-and kaempferol-derivatives from Mongolian oak cups against α-glucosidase, α-amylase and protein glycation linked to type II diabetes and its complications and their influence on HepG2 cells' viability. *Arabian Journal of Chemistry, 11*(8), 1247–1259.

Zengin, G., & Aktumsek, A. (2014). Investigation of antioxidant potentials of solvent extracts from different anatomical parts of *Asphodeline anatolica* E. Tuzlaci: An endemic plant to Turkey. *African Journal of Traditional, Complementary and Alternative Medicines, 11*(2), 481–488.

Zhao, M.-H., Jiang, Z.-T., Liu, T., & Li, R. (2014). Flavonoids in *Juglans regia* L. leaves and evaluation of in vitro antioxidant activity via intracellular and chemical methods. *The Scientific World Journal, 2014*.

Zheng, Y., Yang, W., Sun, W., Chen, S., Liu, D., Kong, X., et al. (2020). Inhibition of porcine pancreatic α-amylase activity by chlorogenic acid. *Journal of Functional Foods, 64*, Article 103587.

Żurek, N., Pycia, K., Pawłowska, A., Potocki, L., & Kapusta, I. T. (2023). Chemical profiling, bioactive properties, and anticancer and antimicrobial potential of *Juglans regia* L. Leaves. *Molecules, 28*(4), 1989.